PCCP

Complexity of globally coupled chaotic electrochemical oscillators

István Z. Kiss,† Wen Wang and John L. Hudson*

Department of Chemical Engineering, University of Virginia, 102 Engineers' Way, PO Box 400741, Charlottesville, VA 22903-2442, USA. E-mail: hudson@virginia.edu

Received 12th May 2000, Accepted 26th June 2000
Published on the Web 31st July 2000

Interactions among small sets of two to eight nickel electrodes undergoing chaotic electrodissolution in sulfuric acid were studied. A single oscillator under these conditions exhibits low-dimensional chaotic behavior. Global coupling among the electrodes was added with the use of external resistors in a manner such that the strength of the coupling could be varied while the other parameters of the system remained constant. Such global coupling is of course equivalent to an appropriate local coupling for the two-electrode system and even for a three-electrode system if arranged in a ring. We investigate the changes in complexities of both the individual oscillators and of the total current as functions of coupling strength and of array size. The dynamics of the individual oscillators are almost identical to those of the single oscillator at added coupling strengths of zero (where the oscillators are almost independent) and at maximum coupling strength (where they are synchronized). There are two trends (with exceptions) with changing coupling strength. (1) The complexity (information dimension) of the individual currents has a maximum at intermediate values of the coupling strength, *i.e.*, at conditions in which interactions occur but where the coupling is not strong enough to produce synchronization. (2) An increase in global coupling decreases the complexity of the total current. The general trends with coupling strength are interrupted by clustering that occurs with the four and eight electrode arrays. Cluster configurations for the larger array exhibiting both chaotic (3,5 cluster) and periodic (4,4 cluster) dynamics were observed.

Introduction

Electrochemical systems exhibit a wide variety of types of dynamical behavior including bistability, periodicity, quasi-periodicity and chaos.[1–6] In the past few years spatiotemporal behavior has received considerable interest.[5] Spatiotemporal structures have been observed during electrodissolution processes (nickel[7] and iron in sulfuric acid,[8,9] cobalt in phosphoric acid[10]), electrocatalytic reactions (reduction of peroxodisulfate,[11] oxidation of formic acid[12]) and deposition processes (silver antimony alloy).[13] Spatiotemporal phenomena such as accelerating fronts, backfiring pulses,[14] rotating waves,[15] traveling and standing waves,[7] spatiotemporal period doublings[8,9] and spirals[13] have been seen.

Spatiotemporal patterns arise through the interaction of nonlinear reaction and coupling among reacting sites. The effect of different types of coupling has been studied numerically[16,17] and in experiments.[12,15,17,18] In electrochemical systems the migration through the electric field in the electrolyte represents a strong long-range coupling between the reacting sites.[19] The role of different types of coupling has been explored by several investigators using small numbers, often two, of interacting electrodes. Wang and Hudson[20] investigated the electrodissolution of two and three iron electrodes embedded in various configurations on the end of a rotating disk and showed that the coupling can lead to chaos and higher dimensional chaos. Nakabayashi *et al.*[21] studied current oscillations of two iron electrodes and proposed that the coupling is mainly through a concentration wave of H^+ ions between the two electrodes. Mukouyama *et al.*[22] found that synchronous current oscillations of the Pt electrodes in H_2O_2–H_2SO_4 solutions are caused by electrical interactions between the oscillating systems. It was shown that migration currents play a major role in the coupling of two oscillating cobalt electrodes in phosphoric acid buffer.[23] The strength of this long-range coupling can be varied through changes in the concentration of the electrolyte and the geometry of the cell. Mukouyama *et al.*[22] changed the distance between the working and reference electrodes in a two-potentiostat setup (H_2O_2 reduction on platinum) and found a distance above which oscillations synchronized. The effect of cell geometry (*i.e.* the orientation of the electrodes and the distance between the working, counter and reference electrodes) has been analyzed.[18,24]

Global coupling is of major importance in many physical[25] and chemical systems.[26] The global nature of coupling serves as a constraint that can produce patterns. An external resistance connected to the working electrode can be used to add a global coupling to an electrochemical system.[27,28] However, the addition of the external resistance will generally also change other conditions such as the driving potential for the reaction. In previous work[29,30] we introduced an experimental setup in which the effect of global coupling can be studied on an array of electrodes without changing other conditions. Altering of the degree of global coupling (and holding all other parameters constant) is done through the use of external resistors; the total external resistance is held constant while the fraction dedicated to individual currents, as opposed to the total current, is varied. In those studies we investigated larger arrays of 64 globally coupled chaotic[30] and periodic[29] oscillators. In the present study we use small sets of from two to eight elements; the nickel/sulfuric acid system is again used. The emphasis here is on the interactions among chaotic oscillators and the effect of the coupling on the complexity of individual and total dynamics. Of course the addition of global coupling is equivalent to the addition of local coupling to sets of two elements and to sets of three elements in a ring-

† Permanent address: Institute of Physical Chemistry, University of Debrecen, Debrecen H-4010, Hungary.

DOI: 10.1039/b003812l

geometry. In the coupling of the sets of four and eight elements, behavior such as cluster formation previously seen in larger systems can already be observed.

Experimental

The specific details of the experiments are described in an earlier paper.[29] An eight-electrode array is used for the experiments (Fig. 1). Each electrode is made from a pure Ni wire (Aldrich Chemical Co., 99.99+%) of diameter 2 mm. The electrodes are embedded in epoxy, and reaction takes place only at the ends. For the experiments one, two (1,5 2,6 3,7 4,8), three (1,2,3 or 5,6,7), four (1,2,5,6 or 3,4,6,7) and eight electrodes were used to study the effect of the increasing number of electrodes.

The electrode array was used as a working electrode in a standard three-electrode electrochemical cell, shown in Fig. 2. The potential of all of the electrodes in the array is held constant using a potentiostat (EG&G Princeton Applied Research, model 273) *vs.* $Hg/Hg_2SO_4/K_2SO_4$ reference electrode. The electrodes are connected to the potentiostat through individual resistors connected to each of the electrodes and one collective resistor. In a few experiments small perturbations of the individual resistors were carried out by a computer-controlled resistor box. Zero resistance ammeters (ZRA's) were used to measure the currents of electrodes independently. Experiments were carried out in 4.5 M H_2SO_4 solution. The counter electrode is a Pt sheet. The cell was thermostated at 11 °C. The resistance of the cell (2 Ω for the three electrodes) is much smaller than the added external resistors (order of 100 Ω).

Dynamics of a single electrode

The Ni/sulfuric acid electrochemical system does not oscillate spontaneously in our setup unless a resistor is connected to the cell.[31,32] If an appropriate external resistance is attached (R_{tot} = 160 Ω) then a steady-state (SS)–period one (P1)–period two (P2)–P1-SS bifurcation structure can be observed with change in the applied potential. With a somewhat higher external resistance (R_{tot} = 200 Ω) a period-doubling route to chaos with a period three window is obtained with change in potential. The chaotic region extends over a range of 20 mV.

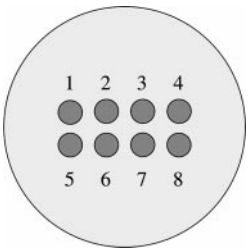

Fig. 1 Schematics of the array.

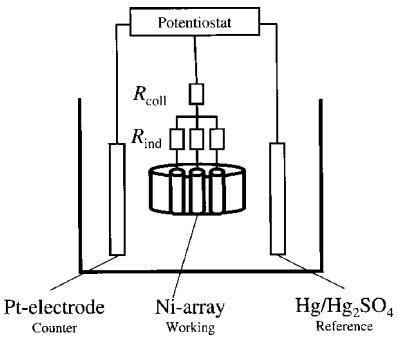

Fig. 2 Experimental setup.

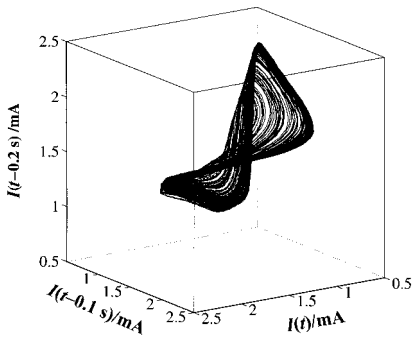

Fig. 3 Reconstructed three-dimensional attractor of the current of the one-electrode setup, V = 1.320 V, R_{eq} = 200 Ω.

An attractor reconstructed from the time series in the chaotic region is shown in Fig. 3.

Coupling parameter

There are two ways of connecting the external resistors to a cell of multiple working electrodes; as shown in Fig. 2, one can add individual resistors (R_{ind}) or collective resistors (R_{coll}). The total resistance is then:

$$R_{tot} = R_{coll} + \frac{R_{ind}}{n} \quad (1)$$

where n is the number of electrodes.

It is sometimes convenient when comparing arrays of different sizes to use an equivalent resistance (R_{eq}); holding R_{eq} constant, and neglecting electrolyte resistance, yields the same double layer potential drop for the same applied potential if the number of electrodes is changed.

$$R_{eq} = nR_{tot} \quad (2)$$

The collective resistance fraction

$$\varepsilon = \frac{R_{coll}}{R_{tot}} \quad (3)$$

is used to characterize the global coupling in the system. If $\varepsilon = 0$, the external resistance furnishes no additional global coupling. If $\varepsilon = 1$, maximal external global coupling is achieved. It should be noted that there is intrinsically in the system, even for $\varepsilon = 0$, some long-range coupling because of potential drops in the electrolyte and in the external circuitry. We thus have a (added) global coupling parameter that takes on values from zero to one as the global coupling increases.

Coupled chaotic oscillators are studied through changing ε while R_{tot} (or R_{eq}) is held constant. This makes it possible to observe the effect of coupling while the other parameters remain unchanged. Series of experiments were carried out with different number of electrodes.

Results

Coupled chaotic oscillators—sets of two and three elements

We first turn to the behavior of very small sets of coupled oscillators. We consider groups of two or three. In addition, the characteristics of the dynamics of the single electrode can be seen again here since both limits of no *added* global coupling ($\varepsilon = 0$) and maximum added global coupling ($\varepsilon = 1.0$) yield individual time series and attractors that are essentially the same as those of a single element. As we shall see below, phenomena such as clustering begin with array sizes as small as four and we therefore discuss separately the results obtained with arrays of size four and eight in the next section.

We begin with the two-electrode configuration. The two time series for both of the electrodes with no global coupling ($\varepsilon = 0$) are shown in Fig. 4a; although the currents are for

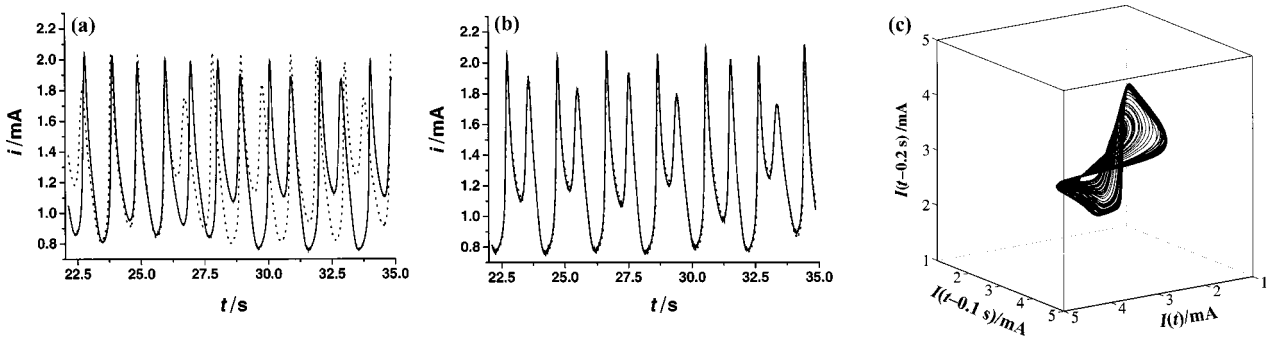

Fig. 4 Two-electrode system, $V = 1.315$ V, $R_{eq} = 260\ \Omega$. (a). Time series of the individual = 0. (b) Time series of the individual currents, $\varepsilon = 1.0$. (c) Attractor reconstructed from time series of total current, $\varepsilon = 1$.

some short times close together, such as around $t = 25$ s in the figure, they diverge in a few oscillations. The two time series for maximal global coupling ($\varepsilon = 1.0$) are shown in Fig. 4b; they are almost identical. Since noise is present, the two time series cannot become exactly identical and we thus define a distance in state space below which we say that the oscillators are synchronized. The attractor constructed from the total current (the sum of the two currents) is seen in Fig. 4c. The attractor of the synchronized system shown in Fig. 4c is *essentially* the same as the attractor of a single uncoupled chaotic attractor, of course with a multiplicative factor of two since the two currents have been added.

Between the two extremes of no global coupling ($\varepsilon = 0$) and maximum global coupling ($\varepsilon = 1.0$) the degree of synchronization increases with increasing coupling. In Fig. 5 we show some results from the three-electrode system. (The two-electrode array results are similar.) We present attractors reconstructed from the current of one of the three electrodes; the time series and the attractors for the three individual electrodes are very similar but do differ quantitatively slightly because of noise and because of heterogeneities in the system. We also calculate the information dimensions from the total current and from one of the individual currents; the dimensions calculated from the three individual electrodes are essentially identical.

The effect of coupling can be seen in the change of the current signals from the individual electrodes as the coupling parameter ε is increased. In Fig. 5a, b and c the attractors reconstructed from the individual time series are shown for $\varepsilon = 0.0$, $\varepsilon = 0.2$ and $\varepsilon = 1.0$ respectively. For no added global coupling the attractor is low-dimensional and unaffected (significantly) by the other elements. The attractors for no coupling and maximum coupling (Fig. 5a and c respectively) are essentially identical. That for an intermediate coupling strength (Fig. 5b) is somewhat distorted.

There are several measures of complexity of time series data (for good surveys see refs. 33 and 34), *e.g.*, different (Hausdorff, correlation, information, Kaplan–Yorke) dimensions, entropies (metric, Kolmogorov, Renyi) and the Lyapunov-spectrum. Of course, it is difficult to characterize the complexity by a single number. The information dimension (D_1) is one measure of the complexity of signals.[35,36] We have chosen D_1 because a robust algorithm exists for estimating it from experimental time series data,[35] implemented in software by Kostelich.[37]

Since we use dimension as one measure of the complexity of the signals, the procedure for calculating D_1 for the total current of the three-electrode setup at $\varepsilon = 0.2$ (Fig. 5b) is presented as an example. A good estimation of D_1 must meet two requirements: adequate scaling and independence of the reconstruction parameters (embedding dimension, m and delay-time, τ) in an acceptable range. For a discussion of the limitations of the algorithms for computing dimension using experimental data see ref. 36 and references therein.

The "fixed mass" method (or nearest neighbor algorithm) calculates the average distance, $\langle \delta_p(k) \rangle$ of the pth neighbor (p is the order of the method) of an 'average' phase point in the attractor based on a random sample of k points. The nearest neighbor distances should scale as

$$\langle \delta(k) \alpha \propto k^{-1/D_1}. \tag{4}$$

The scaling is shown in Fig. 6a on a logarithmic scale for a range of orders. The distances were calculated using 16 000 data points (corresponding to about 100 oscillations). The dimensions were obtained by fitting a line to the rightmost ten points in the curves and making an average for $30 \leqslant p \leqslant 90$. At $p = 10$ the dimensions were usually larger, probably due to the effect of noise. Fig. 6a was determined using an embedding dimension of 7 with a delay time of 0.175 s. The effects of both reconstruction parameters are discussed below.

The choice of an appropriate delay is important to the success of reconstruction. One approach is to compute the correlation function of the time series data. Since the system is chaotic, the autocorrelation function decreases with time

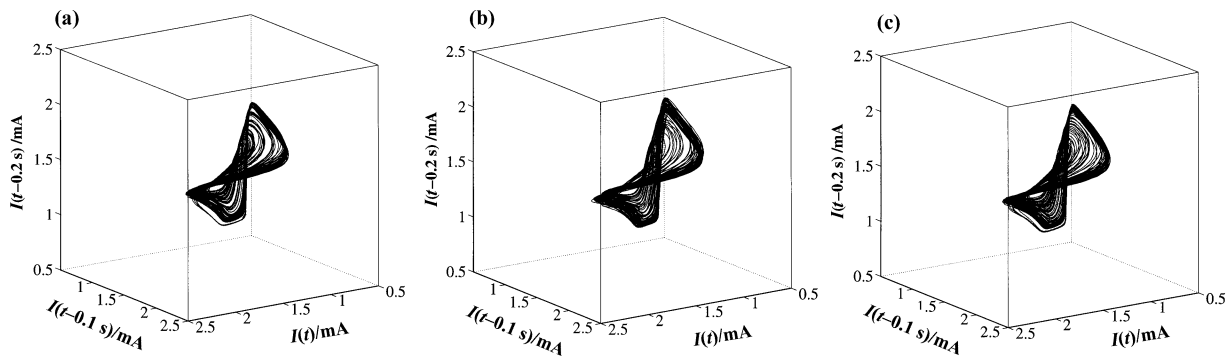

Fig. 5 Attractors reconstructed from current of one electrode. Three-electrode system, $V = 1.340$ V, $R_{eq} = 300\ \Omega$. (a) $\varepsilon = 0$, (b) $\varepsilon = 0.2$, (c) $\varepsilon = 1.0$.

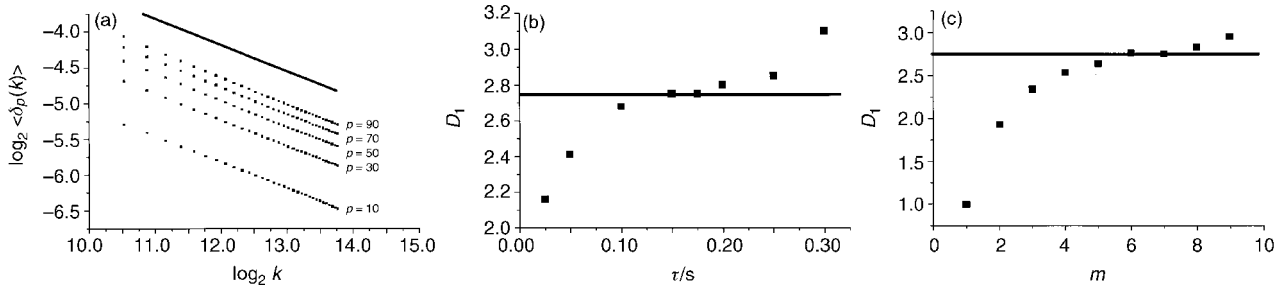

Fig. 6 Calculation of information dimension for a time series of the total current for a three-electrode setup at $\varepsilon = 0.2$ (other parameters are as in Fig. 5). The solid line in the figures represents the determined dimension of 2.74. (a) The scaling law of eqn. 4 at different orders (p). Embedding parameters: $m = 7$ and $= 0.175$ s (b) The effect of the delay-time on the calculated dimensions at a fixed embedding dimension of 7. (c) The effect of embedding dimension on the calculated dimensions at a fixed delay-time of 0.175 s.

separation. The first zero crossing time (T_0) is indicative of the time scale of the system for which there is no correlation between the data points. Therefore a modest fraction of T_0 is a good first approximation of proper τ.[34] In the present case $T_0 = 0.26$ s. In Fig. 6b the dimensions obtained are shown as τ is varied. With increasing τ the dimensions increase; however, in the range $0.1\ \text{s} \leqslant \tau \leqslant 0.2$ s the increase is small. Close to $T_0(0.2\ \text{s} < \tau)$ the dimensions increase again due to the small correlation. Based on these results the delay-time for calculating the dimensions was chosen to be 0.175 s.

The proper choice of the embedding dimension is another concern. It is important that the reconstruction be embedded in a space of sufficiently large dimension to represent the dynamics completely. The variation of D_1 as a function of the embedding dimension (m) is shown in Fig. 6c. At low values of m the dimension is equal to the embedding dimension. With increasing m the dimensions increase and reach a reasonable value of 2.74 if $5 \leqslant m \leqslant 8$. In this case $m = 5$ gives a proper value for dimension, however, we applied $m = 7$ in all the calculations presented so that the results for larger arrays can be easily compared to that of the smaller ones. (A larger dimension requires a larger embedding.)

One reference point for checking the calculation is the value of D_1 for a periodic orbit. We have obtained $D_1 = 1.1$ for the periodic attractor presented later in Fig. 10a. In theory, the dimension of a periodic orbit should be 1. The slight increase of D_1 might result from an error of the relatively complex structure of the periodic orbit (period-6) amplified by noise.

We have carried out a countercheck of the applied algorithm using methods from the software package "TISEAN".[38] Similar values were obtained for D_1 (using the c1 program), *e.g.* for the total current of the three-electrode setup at $\varepsilon = 0.2$ the value is 2.82. Based on the presented results the error of dimensions is about 0.1. We also calculated some of the dimensions using the correlation dimension (D_2) calculation algorithm of TISEAN (program d2). Again, similar values and trends were obtained. For the representative time-series data (Fig. 5b) we obtained $D_2 = 2.76$. In theory, $D_2 \leqslant D_1$ (if the points are uniformly distributed on the fractal equality holds); however, in practice the numerical values are usually close to each other.[39]

The information dimension of a signal from an individual element of the three-electrode array as a function of coupling strength is shown in Fig. 7a. At both $\varepsilon = 0$ and $\varepsilon = 1.0$ it has a value of approximately 2.3. A similar value of D_1 was calculated for the one-electrode system. Thus the dynamics of the almost uncoupled case ($\varepsilon = 0$) and the synchronized case ($\varepsilon = 1.0$) are similar. However, the dynamics are more complicated at intermediate values of the coupling strength where interactions occur but where synchronization has not been attained. The information dimension of the individual signal goes through a maximum at $\varepsilon = 0.2$ as is seen in Fig. 7a. Such a maximum in the dimension reconstructed from the time series of an individual element occurs for all array sizes; the value of coupling strength at which the maximum occurs becomes larger as the number of electrodes in the array becomes greater, at least up to eight elements for which the results here are presented. For arrays of two and three elements the maximum occurs at $\varepsilon = 0.2$, for four elements it occurs at $\varepsilon = 0.44$ and for eight elements it occurs at $\varepsilon = 0.6$. (Note, however, that a complicating factor arises for larger arrays, *viz.*, the occurrence of clusters; this alters the dependency of the dimension on the coupling parameter. Periodic behavior can occur. The arrays of four and eight electrodes are discussed in more detail in the next section.)

The information dimension of the signal from the total current is shown in Fig. 7b. The total current or total rate of reaction is often the quantity of particular importance in an experiment and sometimes the only quantity measured. The complexity of the total current is determined by three factors: (a) the complexity of the individual elements, (b) the correlation between the elements and (c) the number of elements. As the coupling is increased the complexity of individual elements generally goes through a maximum while the correlation generally increases (resulting in a decrease of total complexity). In the experiments as the coupling is increased the information dimension of the attractors reconstructed from the total current decreases monotonically and reaches its minimum value of about 2.3 at a value of ε approximately equal to 0.3–0.4 as seen in Fig. 7b.

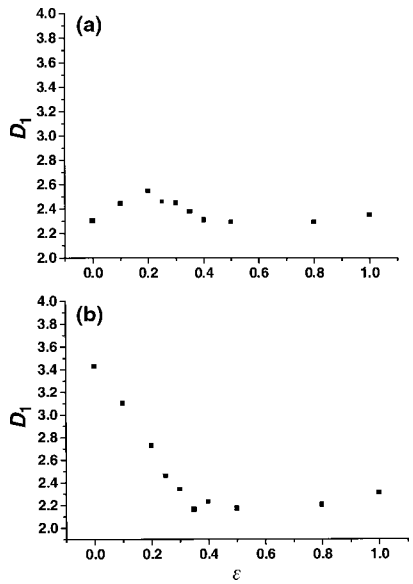

Fig. 7 Information dimension of attractors as a function of global coupling (delay-time and the embedding dimension of the reconstruction are 0.175 s and 7, respectively). Three-electrode setup (other data are as in Fig. 5). (a) Dimensions from the current of electrode #1. (b) Dimensions from total current.

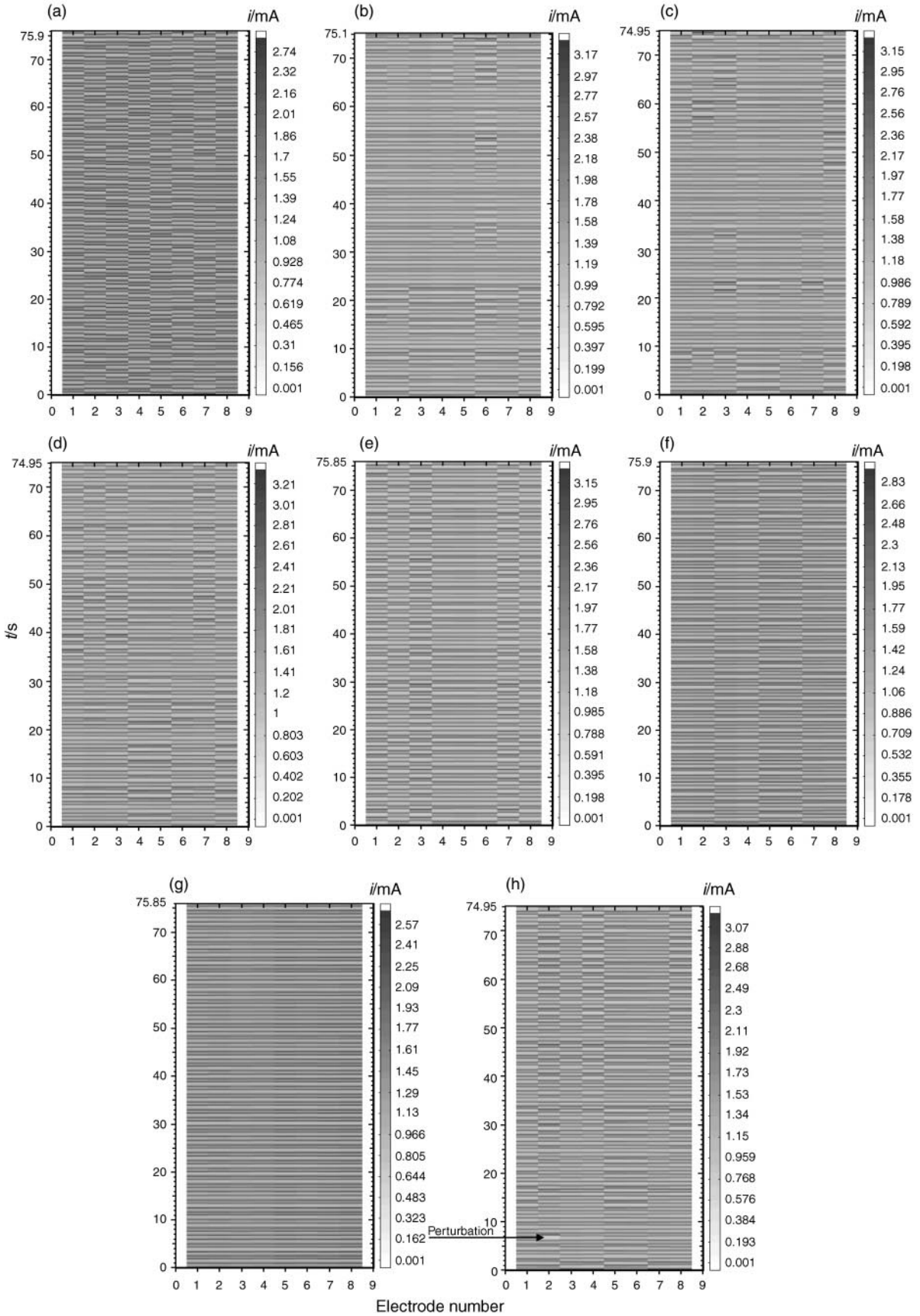

Fig. 8 Space–time plot of the local currents of the eight-electrode array; dark corresponds to high current. $V = 1.350$ V, $R_{eq} = 200$ Ω. (a) $\varepsilon = 0$, (b) $\varepsilon = 0.65$, (c) $\varepsilon = 0.675$, (d) $\varepsilon = 0.7$, (e) $\varepsilon = 0.725$, (f) $\varepsilon = 0.725$, (g) $\varepsilon = 1$, (h) $\varepsilon = 0.725$. Transition between the (4,4) and (3,5) cluster configurations induced by perturbation of electrode #2.

Coupled arrays of 4 and 8 elements

In the case of arrays of 4 and 8 elements there are some deviations from the trends observed with the smaller arrays as coupling is varied. The complexity of individual current again goes through a maximum. The information dimension of total current has a decreasing trend but the decrease is not as steep as for the three-electrode case and a plateau is observed in the range $\varepsilon = 0.4$–0.6 indicating that the synchronizing effect of

global coupling is offset by the effect of increased dimension of the individual currents.

The general trends are interrupted by clustering that occurs for intermediate values of the coupling strength in the four- and eight-electrode systems. (Clustering has been observed even in a three-element system of coupled periodic oscillators.[29])

We present some results for the eight-electrode system. (Those for four electrodes are qualitatively similar and thus are not shown.) Space–time plots are shown in Fig. 8 for various values of the coupling strength; the dark shading corresponds to higher current. Some time series, in each case the difference between the signals of two elements, are shown in Fig. 9.

For $\varepsilon = 0$ the elements oscillate almost independently (Fig. 8a) and for $\varepsilon = 1.0$ they are synchronized (Fig. 8g). At an intermediate value of coupling ($\varepsilon = 0.725$) clusters form. Two cluster configurations (3,5)—that is with three elements in one cluster and five in the other—and (4,4) can be seen in Fig. 8e and f respectively. Since these results are for an array of only eight elements, the number of possible cluster configurations is limited. We have only seen (3,5) and (4,4). In the cluster region, depending on initial conditions, either of the two possible configurations is seen. Of course the specific elements in a given cluster change. The difference between the signals of two of the elements in the cluster region is shown in Fig. 9a (elements in different clusters) and in Fig. 9b (elements in the same cluster). Note again that the difference between the signals of the elements in the same cluster is small, but not identically zero. It is possible with short disturbances (perturbations of duration of one second were imposed with a computer controlled resistor) to change the cluster configuration. Since the configurations are very stable, a small disturbance will not effect such a change. (The elements remain in the cluster configuration without external perturbation for the duration of the experiment.) The result of such a disturbance is shown in Fig. 9c. The initial configuration is a (4,4) cluster. The difference between the signals of two elements in the same cluster can be seen. The difference is approximately zero without disturbance. A small disturbance is added at $t = 25$ s on electrode #2. After a short transient the system returns to its initial state. A somewhat greater perturbation is introduced at $t = 40$ s. Again the system returns to its initial state. Finally at $t = 60$ s a sufficiently large disturbance produces a transition from one cluster to the other and a configuration change from (4,4) to (3,5). The configuration change did not occur by the movement of the perturbed element from one cluster to the other (see Fig. 8h). Three electrodes, #2 (the perturbed one), #3 and #7 changed clusters and in this case the net total change was one, *i.e.*, a change occurred from (4,4) to (3,5). The change of configuration results in a change of dynamics of the individual elements as well. Attractors reconstructed from time series of one element of the (4,4) and of the

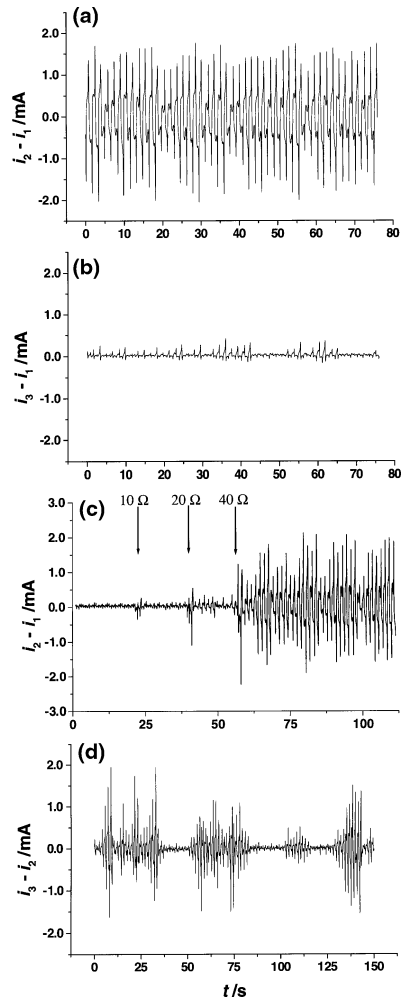

Fig. 9 Differences between currents on two electrodes. Eight-electrode, array. $V = 1.350$ V, $R_{eq} = 200$ W, (a) $\varepsilon = 0.725$, electrodes not in same cluster, (b) $\varepsilon = 0.725$, electrodes in same cluster, (c) $\varepsilon = 0.725$, transitions induced by perturbation of the individual resistors of electrode #2 (the resistance was increased by the value shown for a period of 1 s), (d) $\varepsilon = 0.675$, transient cluster region.

(3,5) configurations are shown in Fig. 10. The dynamics of the element of (4,4) configuration is periodic while that of the (3,5) configuration is banded chaotic. The banded nature is more clearly seen in the two dimensional projection of the attractor shown in Fig. 10c.

Consider now the behavior of the eight-element array at values of coupling strength just below that at which clustering occurs. Some space–time plots are shown in Fig. 8b, c and d. This is a region of transient cluster formation. The clusters

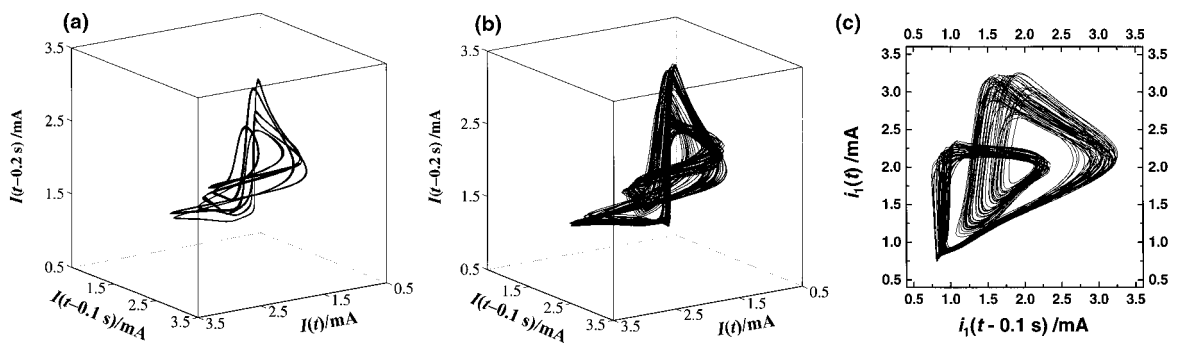

Fig. 10 Attractors reconstructed from time series of one element in the cluster region. (a) (4,4) configuration (b) (3,5) configuration. (c) Projection of (3,5) attractor.

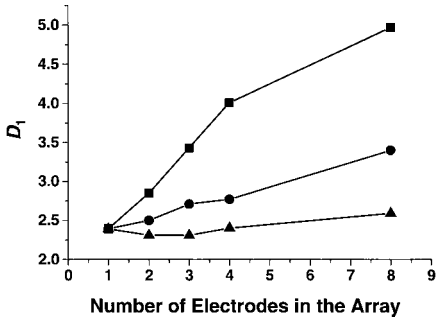

Fig. 11 Information dimension of the attractors reconstructed from the total current as a function of the numbers of electrodes in the array for $\varepsilon = 1$ (triangles), $\varepsilon = 0.2$ (circles) and $\varepsilon = 0$ (squares).

form but are not stable and thus with time break up. The length of time during which the clusters remain intact before breaking up increases as the coupling strength approaches that at which stable clusters occur. The difference in two signals in this region is shown in Fig. 9d. Note that during some periods the two elements are in a cluster but that there are intermittent regions where the elements are not synchronized.

We note that statistical methods have been applied to the cluster region using arrays of 64 electrodes.[30]

The third factor that determines the complexity of total current is the number of elements in the array. The information dimension reconstructed from the total current as a function of the number of elements is shown in Fig. 11 at three fixed values of the coupling parameter ε. (Note that values of ε are chosen outside the cluster region.) For maximum coupling ($\varepsilon = 1.0$) the electrodes are synchronized for all array sizes. In this case the array acts as a single electrode and hence the dimension calculated from the total current is approximately independent of the number of electrodes in the array. The information dimension has a value of approximately 2.3 for all array sizes. With weaker coupling ($\varepsilon = 0.2$) the dimension does increase as the number of electrodes increases. There is an approximately linear increase in dimension from about 2.3 to about 3.3 as the array size is increased from 1 to 8 elements. With no added coupling ($\varepsilon = 0.0$) the increase in dimension is of course greater than in the presence of coupling. Nevertheless, the rise is not as great as it would be theoretically in a system without coupling. In that latter case the dimension would scale linearly and proportionally with array size. (Of course the accuracy of the dimension calculation becomes poorer as the value of the dimension increases; nevertheless, it is clear from the results obtained with one to four electrodes that the increase in the dimension as the size is increased from one to four is less than the factor of four that would be expected theoretically without coupling.) The lower value is at least partially attributed to the presence of the small amount of coupling inherent in the system with no added global coupling ($\varepsilon = 0$). This coupling arises largely from potential drops in the electrolyte (yielding migration) and in the external circuitry.

Concluding remarks

The effect of coupling on small sets (two to eight) of chaotic oscillators was studied. The imposed coupling was global, *i.e.*, each element influences all other elements equally. The oscillators, without coupling, exhibited low-dimensional chaotic behavior. As in any experiment, there is a small amount of heterogeneity and noise present in the system.

Global coupling is equivalent to an appropriate local coupling for the two-electrode system and even for a three-electrode system if arranged in a ring. Thus these results add to the studies in the literature on coupled chaotic systems, many of which are performed with two elements.

Another area of recent investigation is synchronization and cluster formation in large sets of chaotic oscillators. Many simulations using coupled chaotic maps[25] and differential equations[40] have been reported; such simulations are typically performed on larger lattices. Some experimental studies have been reported using the nickel–sulfuric acid system on arrays of 64 electrodes.[30] The results in the present paper using the four- and eight-electrode arrays cannot be used to develop statistical information but can be used to observe the occurrence of some behavior such as the clustering that has been seen in the larger systems.

The dynamics of the system can be viewed from two viewpoints, that of the individual oscillators and that of the entire system. In the first then we are looking at the effect of coupling on the dynamics of oscillators. The second viewpoint is one of observations of the entire system in the sense that an array of electrodes has been shown to give qualitatively similar overall dynamics as a larger single electrode. An interface can sometimes be thought of as a collection of oscillators acting in parallel.[41] (Of course the detailed structure on a spatial scale of the size of the elements in the array is going to be different from that of a single, larger electrode; the similarity is on the scale of the larger electrode or entire array.[42]) In this sense one is interested in the total current or rate of reaction.

The global coupling was imposed over a range from almost no coupling to that which produced synchronization. Therefore, both without added coupling and with maximum global coupling the dynamics of the individual oscillators were essentially those of a single element.

For any given (fixed) array size as the coupling strength is increased from zero the overall or total current dynamics become simpler; however, the individual currents become more complex (the time series become more chaotic and the attractor dimensions increase). In the case of two- and three-electrode systems, with further increase of coupling strength the dimensions of the individual currents go through maxima before returning to the value of a single oscillator. The complexity of the total current decreases monotonically with increasing coupling.

With four- and eight-electrode systems the general trends still are found except in an intermediate region of coupling strength in which clustering occurs. All the elements in a given cluster have essentially the same temporal dependence and thus follow the same trajectory in state space. However, the two clusters follow different paths. Two different cluster configurations, (4,4) and (3,5) states, were seen in the experiments. The first of these is periodic and the second is chaotic. Kaneko has discussed the dependency of the dynamics on cluster size for the two-cluster configuration in his investigations of 1000 coupled maps;[25] he presents a bifurcation diagram as a function of cluster size. In our experiments with eight electrodes, we see only two cluster sizes. We have not seen clusters with configurations (2,6) or (1,7); it is likely that these states are not stable although it is possible that they are stable but have a small basin of attraction. Clusters in the range (18,46) to (32, 32) have been observed in similar experiments with arrays of 64 electrodes.[30] Multiple stable states thus do exist under the same conditions and the state that is attained depends on the initial conditions. We were able to perturb the system from one cluster state to another with a sufficiently large disturbance. We did not look for hysteresis in the system through changes in the parameters, the applied potential or the coupling strength; however, hysteresis has been observed in studies with two coupled chaotic CSTRs as the coupling strength was increased and decreased.[43,44] We note that the multiple states that exist at the same conditions exhibit differences not only

in the dynamics of the individual oscillators but also in the overall current or rate of reaction.

Acknowledgements

This work was supported by the National Science Foundation and by the Fulbright Hungarian–American Exchange Program.

References

1 J. Wojtowicz, in *Modern Aspects of Electrochemistry*, ed. J. O. Bockris and B. E. Conway, Butterworth, London, 1973.
2 J. L. Hudson and T. T. Tsotsis, *Chem. Eng. Sci.*, 1994, **49**, 1943.
3 M. T. M. Koper, *Adv. Chem. Phys.*, 1996, **92**, 161.
4 M. T. M. Koper, *J. Chem. Soc., Faraday Trans.*, 1998, **94**, 1369.
5 K. Krischer, in *Modern Aspects of Electrochemistry*, ed. J. O. Bockris, B. E. Conway, and R. E. White, Plenum Press, NY, 1998, vol. 32.
6 J. L. Hudson, *IMA Volume in Mathematics and its Applications 115*, ed. M. Golubitsky, D. Luss and S. H. Strogatz, Springer, New York, 1999, vol. 137.
7 O. Lev, M. Sheintuch, L. M. Pismen and H. Yarnitzky, *Nature*, 1988, **336**, 458.
8 J. L. Hudson, J. Tabora, K. Krischer and I. G. Kevrekidis, *Phys. Lett. A*, 1994, **179**, 355.
9 J. C. Sayer and J. L. Hudson, *Ind. Eng. Chem. Res.*, 1995, **34**, 3246.
10 R. D. Otterstedt, N. I. Jaeger and P. J. Plath, *Int. J. Bifurcation Chaos*, 1994, **4**, 1265.
11 G. Flätgen and K. Krischer, *Phys. Rev. E*, 1995, **51**, 3997.
12 J. Christoph, P. Strasser, M. Eiswirth and G. Ertl, *Science*, 1999, **284**, 291.
13 I. Krastev and M. T. M. Koper, *Physica A*, 1995, **213**, 199.
14 R. D. Otterstedt, P. J. Plath, N. I. Jaeger, J. C. Sayer and J. L. Hudson, *Chem. Eng. Sci.*, 1996, **51**, 1747.
15 R. D. Otterstedt, P. J. Plath, N. I. Jaeger and J. L. Hudson, *J. Chem. Soc., Faraday Trans.*, 1996, **92**, 2933.
16 N. Mazouz, K. Krischer, G. Flätgen and G. Ertl, *J. Phys. Chem. B*, 1997, **101**, 2403.
17 J. Christoph, R. D. Otterstedt, M. Eiswirth, N. I. Jaeger and J. L. Hudson, *J. Chem. Phys.*, 1999, **110**, 8614.
18 P. Grauel, J. Christoph, G. Flätgen and K. Krischer, *J. Phys. Chem. B*, 1998, **102**, 10264.
19 U. F. Franck and L. Meunier, *Z. Naturforsch. B*, 1953, **8**, 396.
20 Y. Wang and J. L. Hudson, *J. Phys. Chem.*, 1992, **96**, 8667.
21 S. Nakabayashi, K. Zama and K. Uosaki, *J. Electrochem. Soc.*, 1996, **143**, 2258.
22 Y. Mukouyama, H. Hommura, T. Matsuda, S. Yae and Y. Nakato, *Chem. Lett.*, 1996, 463.
23 J. C. Bell, N. I. Jaeger and J. L. Hudson, *J. Phys. Chem.*, 1992, **96**, 8671.
24 N. Mazouz, G. Flätgen and K. Krischer, *Phys. Rev. E*, 1997, **55**, 2260.
25 K. Kaneko, *Physica D*, 1990, **41**, 137.
26 G. Veser, F. Mertens, A. S. Mikhailov and R. Imbihl, *Phys. Rev. Lett.*, 1993, **71**, 935.
27 R. D. Otterstedt, N. I. Jaeger, P. J. Plath and J. L. Hudson, *Chem. Eng. Sci.*, 1999, **54**, 1221.
28 N. Mazouz, G. Flätgen, K. Krischer and I. G. Kevrekidis, *J. Electrochem. Soc.*, 1998, **145**, 2404.
29 I. Z. Kiss, W. Wang and J. L. Hudson, *J. Phys. Chem. B*, 1999, **103**, 11433.
30 W. Wang, I. Z. Kiss and J. L. Hudson, *Chaos*, 2000, **10**, 248.
31 O. Lev, A. Wolffberg, M. Sheintuch and L. M. Pismen, *Chem. Eng. Sci.*, 1988, **43**, 1339.
32 O. Lev, A. Wolffberg, L. M. Pismen and M. Sheintuch, *J. Phys. Chem.*, 1989, **93**, 1661.
33 E. Ott, in *Chaos in Dynamical Systems*, Cambridge University Press, Cambridge, 1994.
34 G. L. Baker and J. P. Gollup, in *Chaotic Dynamics: An Introduction*, Cambridge University Press, Cambridge, 1996.
35 R. Badii and A. Politi, *J. Stat. Phys.*, 1985, **40**, 725.
36 E. J. Kostelich and H. L. Swinney, in *Chaos Related Nonlinear Phenomena*, ed. I. Procaccia and M. Shapiro, Plenum, New York, 1987.
37 E. J. Kostelich, *Software for calculating attractor dimension using the nearest neighbor algorithm*, Department of Mathematics, Arizona State University, AZ, 1990.
38 R. Hegger, H. Kantz and T. Schreiber, *Chaos*, 1999, **9**, 413.
39 P. Grassberger and I. Procaccia, *Physica D*, 1983, **9**, 189.
40 D. H. Zanette and A. S. Mikhailov, *Phys. Rev. E*, 1998, **57**, 276.
41 J.-N. Chazalviel and F. Ozanam, *J. Electrochem. Soc.*, 1992, **139**, 2501.
42 Z. Fei, B. J. Green and J. L. Hudson, *J. Phys. Chem. B*, 1999, **103**, 2178.
43 M. Dolnik and I. R. Epstein, *Phys. Rev. E*, 1996, **54**, 3361.
44 M. J. B. Hauser and F. W. Schneider, *J. Chem. Phys.*, 1994, **100**, 1058.